Chem. Mater. 1991, 3, 898–902

Ion-Beam Studies of the Intercalative Ion-Exchange Mechanism in Muscovite Mica

Vivek Mehrotra and Emmanuel P. Giannelis*

Department of Materials Science and Engineering, Cornell University, Ithaca, New York 14853

Received April 8, 1991. Revised Manuscript Received June 25, 1991

The intercalative ion-exchange properties of mica have been studied by using Rutherford backscattering spectrometry. Reaction of muscovite mica with $AgNO_3$ by the vapor-transport method or from the liquid melt results in a gradual replacement of potassium by silver cations. The concentration gradient observed for the silver cations is attributed to a reaction mechanism wherein ion-exchange progresses by intercalating successive galleries through the edges of the mica layers.

Introduction

Despite the large number of studies devoted to intercalation of mica-type silicates (MTSs), very little is known about the intercalation or ion-exchange properties of mica. This is because micas are considered to be relatively inert to both intercalation and ion exchange. They belong to the general family of 2:1 layered silicates in which two silicic acid sheets are fused to an edge-shared octahedral sheet of aluminum hydroxide or magnesium hydroxide[1,2] (Figure 1). The former arrangement is usually found in the mineral muscovite, and the latter is common in phlogopite. Isomorphous substitution of silicon by aluminum results in a positive charge deficiency, denoted by x, where x equals the charge density per unit cell. The unit cell is equivalent to an Si_8O_{20} unit. The charge deficiency is generally balanced by potassium cations that reside in the galleries between the layers of the 2:1 structure. In "ideal" micas the stoichiometry is such that the potassium ions occupy all the ditrigonal cavities formed by the oxygen atoms of the tetrahedral sheet of the layers.

Micas with $x = 2$ and the talc–pyrophyllite group ($x = 0$) represent the end members of a hierarchy defined by the degree of layer charge density. MTSs or swelling silicates with layer charge densities between $0 < x < 2$ define a separate family of host lattices with physical and chemical properties not found in the end members.[1] For example, unlike the micas, the swelling silicates can intercalate a large number of polar molecules in their galleries with a substantial increase in the gallery height. In addition, it is generally accepted that micas do not exhibit any significant cation-exchange capacity that is common for the intermediate members.

In fact, new functionalities can be introduced in MTSs by simple intercalative or ion-exchange procedures so that the properties of MTSs can be easily fine-tuned.[3] In contrast, micas seem to be relatively inert to such processes, thus limiting their potential application as host lattices. This is a real disadvantage in view of the very attractive properties of mica such as optical transparency and the availability of very large size crystals of good quality. In addition, layered silicates have been recently recognized as an intriguing new system for studying intercalation and quasi-two-dimensional physics.[4–6] These studies, presently limited by the availability of single crystals, will be greatly enriched if micas were amenable to intercalation.

We report here the first observation of an ion-exchange reaction in mica by the vapor-transport method. Rutherford backscattering spectrometry (RBS) is used to obtain chemical compositions following the reaction. RBS has been used before to estimate the bulk and surface cation concentration in zeolites.[7,8] A reaction mechanism wherein intercalation and ion-exchange progress by decorating successive galleries in a manner similar to that observed in graphite[9,10] is being proposed.

In graphite, intercalation proceeds because of a charge transfer between the intercalant and the end basal planes. As a result the nth space is intercalated, where n is the stage number.[10] The effect is subsequently transferred through the galleries until intercalation is complete. The intercalation process is countered by the energy required to distort two adjacent atomic planes.

Our work was motivated by previous reports on photoinduced effects in $AgNO_3$–mica intercalation compounds.[11,12] The remarkable discovery of photochromism and optical switching was attributed to a stage-2 intercalation in which one layer of intercalant ($AgNO_3$) is alternately stacked with two mica layers. The formation of stage-2 intercalation compound with mica seemed unusual not only because micas were believed to be relatively inert toward intercalation but also because the stacking sequence in MTSs is always stage-1.[4]

We have found, instead, that silver is incorporated in mica by an intercalative ion-exchange mechanism. Using

---

(1) Pinnavaia, T. J. *Science* **1983**, *220*, 365.

(2) Pinnavaia, T. J. In *Chemical Physics of Intercalation*; Legrand, A. P., Flandrois, S., Eds.; Plenum Press: New York, 1987; pp 233–252.

(3) (a) Thomas, J. M. In *Intercalation Chemistry*; Whittingham, M. S., Jacobson, A. J., Eds.; Academic Press: New York, 1982; pp 55–99 and references therein. (b) Laszlo, P. *Science*, **1987**, *235*, 1473. (c) Suib, S. L.; Carrado, K. A. *Inorg. Chem.* **1985**, *24*, 863. (d) Newsham, M. D.; Giannelis, E. P.; Pinnavaia, T. J.; Nocera, D. G. *J. Am. Chem. Soc.* **1988**, *110*, 3887. (e) Giannelis, E. P. *Chem. Mater.* **1990**, *2*, 627. (f) Giannelis, E. P.; Mehrotra, V.; Russell, M. W. In *Better Ceramics Through Chemistry*; Brinker, C. J., Clark, D. E., Ulrich, D. R., Zelinski, B. J. J., Eds.; MRS Proceedings; Materials Research Society: Pittsburgh, PA, 1990; Vol. 180, p 685. (g) Mehrotra, V.; Giannelis, E. P. *Solid State Commun.* **1991**, *77*, 155.

(4) Solin, S. A. In *Intercalation in Layered Solids*; Dresselhaus, M. S., Ed.; Plenum Press: New York, 1986; pp 145–154.

(5) Cai, Z.-X.; Mahanti, S. D.; Solin, S. A.; Pinnavaia, T. J. *Phys. Rev. B* **1990**, *42*, 6636.

(6) Wada, N.; Hines, D. R.; Ahrenkiel, S. P. *Phys. Rev. B* **1990**, *41*, 12895.

(7) Baumann, S.; Strathman, M. D.; Suib, S. L. *J. Chem. Soc., Chem. Commun.* **1986**, 308.

(8) Baumann, S. A.; Strathman, M. D.; Suib, S. L. *Anal. Chem.* **1988**, *60*, 1046.

(9) Hooley, J. G. *Mater. Sci. Eng.* **1977**, *31*, 17.

(10) Bartlett, N.; McQuillan, B. W. In *Intercalation Chemistry*; Whittingham, M. S., Jacobson, A. J., Eds.; Academic Press: New York, 1982; pp 19–53 and references therein.

(11) Kambe, N.; Yamada, T. *Appl. Phys. Lett.* **1983**, *43*, 878.

(12) Kambe, N.; Yamada, T. In *Defect Properties and Processing of High-Technology Non-Metallic Materials*; Crawford, J. H., Jr., Chen, Y., Sibley, W. A., Eds.; Elsevier: New York, 1984; pp 467–473.

0897-4756/91/2803-0898$02.50/0

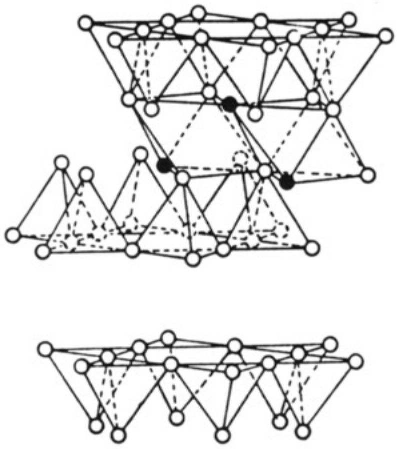

Figure 1. Idealized structure for 2:1 layered silicates showing two tetrahedral sheets sandwiching an octahedral sheet. Open circles represent oxygen atoms; closed circles are hydroxyl groups. In mica the galleries between the layers are usually occupied by potassium cations.

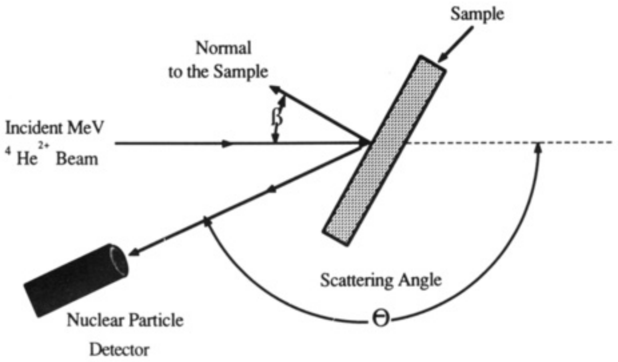

Figure 2. Experimental geometry for Rutherford backscattering spectrometry (RBS).

ion-beam analysis, we have found that the concentration of Ag^+ ions decreases from the surface to the interior of the sample. The concentration gradient is attributed to a reaction mechanism, in which ion exchange proceeds via intercalation of successive galleries wherein the interlayer potassium ions are gradually replaced by silver ions.

Theory and Experimental Technique

The RBS technique, with the experimental geometry shown in Figure 2, measures the energy of ions that are elastically backscattered after impinging on a sample.[13] Particularly, in this work, a beam of He^{2+} ions of energy E_0 is directed toward the sample at an angle β with respect to the sample surface. The subsequent collision of the beam with the target results in He^{2+} ions backscattered by elastic collisions with nuclei in the target. The energy of the backscattered ions is measured by using a silicon surface barrier detector placed at an angle θ with respect to the incident beam. In the RBS experiment, a current pulse proportional to the particle energy is produced when a particle reaches the detector. The magnitude of the signal is measured and registered as counts in successive intervals (channels).

Since the collisions are elastic, both the energy and momentum are conserved in the collision. The energy E_1 of the backscattered He^{2+} ions is related to its energy before collision, E_0, by

$$E_1 = KE_0 \qquad (1)$$

where the kinematic factor K for target nuclei heavier than He is given by

$$K = \{[1 - (m\ (\sin\theta)/M)^2]^{0.5} + m\ (\cos\theta)/M\}^2/(1 + m/M)^2 \qquad (2)$$

where m and M are the masses of the He^{2+} and the target nuclei, respectively, and θ is the scattering angle as shown in Figure 2.

Since the kinematic factor for heavier atoms is greater than that for lighter ones, peaks at high energy correspond to heavier nuclei. The areas and heights of peaks corresponding to different nuclei will be quite different since the scattering probability (cross section) is given by

$$\sigma = (e^2zZ/4E)^2[\sin^{-4}(\theta/2) - 2(m/M)^2 + \ldots] \qquad (3)$$

where z and Z are the atomic numbers of the He ions and the target nuclei, respectively, and E is the energy of He ions just before the collision.

He^{2+} backscattered by a nucleus significantly below the surface of the sample will emerge with less energy than the one scattered by a similar nucleus at the surface due to additional energy losses by inelastic electron collisions. The energy loss of the particle, dE/dx, can be calculated from its stopping cross section $\epsilon(E)$ by[13]

$$dE/dx = \epsilon(E)N \qquad (4)$$

where N is the atomic density (atoms/cm^3) of the target. Cross-section values are tabulated for pure elements and can be easily converted to those for compounds or molecules using Bragg's rule.[14]

The yield of ions scattered from a target element corresponding to the height of the peak, H, is given by

$$H = \sigma\Omega QA \qquad (5)$$

where σ is the scattering cross section as defined above, Ω is the detector solid angle, Q is the number of incident ions, and A (atoms/cm^2) is the areal density. RBS spectra are plots of yield versus energy of the scattered ions in a fixed geometry.

The expected RBS spectrum for a specimen with a certain composition can be simulated with a computer program.[15] Chemical compositions are obtained with an accuracy of 1%, especially for heavier elements.[16] Figure 3, top, shows the simulated spectrum of partially exchanged Ag–mica (1 Ag ion/unit cell) uniformly distributed throughout the sample. Note the step feature observed from the silver scattering. However, a quite different RBS spectrum is obtained if the concentration of Ag varies with depth (Figure 3, bottom). In the simulated spectrum, the number of Ag ions at the surface is set equal to one per unit cell, the diffusion is assumed to be Fickian, and the product of the diffusion coefficient and time is 4.3×10^{-7} cm^2. The rapid decrease in the yield of He^{2+} ions, scattered from Ag, with decreasing energy reflects the decrease in the concentration of Ag ions with depth.

Experimental Section

The ion-exchange reaction was carried out by the vapor-transport method as described previously in the literature[11,12] or from the liquid melt. The muscovite mica samples ($10 \times 10 \times 0.5$ mm^3) were freshly cleaved and loaded with the $AgNO_3$ into a quartz tube. The tube was evacuated to ca. 10^{-6} Torr, sealed,

---

[13] Feldman, L. C.; Mayer, J. W. *Fundamentals of Surface and Thin Film Analysis*; North-Holland: New York, 1986.

[14] Marion, J. B.; Young, F. C. *Nuclear Reaction Analysis, Graphs and Tables*; Wiley: New York, 1968.

[15] Doolittle, L. *Nucl. Instrum. Methods* **1985**, *B9*, 344.

[16] Leavitt, J. A.; McIntyre, L. C.; Ashbaugh, M. D.; Dezfouly, B.; Oder, J. G. *Appl. Opt.* **1989**, *28*, 2762.

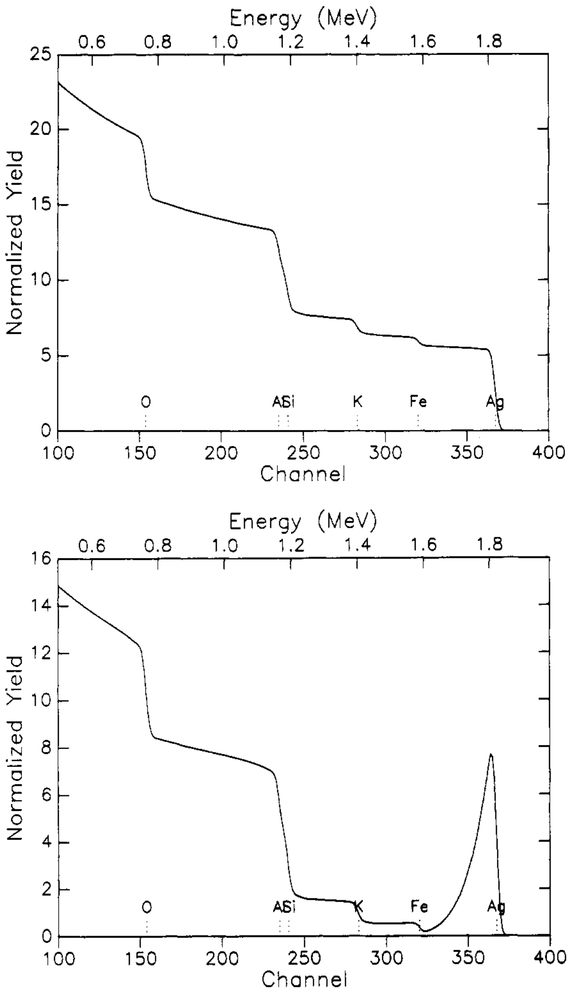

Figure 3. Simulated RBS spectra from a mica sample in which half of the potential ion-exchange sites have been occupied by Ag. Top: the concentration of silver is uniform throughout the sample. Bottom: a diffusion gradient with a *Dt* product of 4.3 × 10^{-7} cm^2 is assumed.

and heated to 350 °C for various time intervals. After certain reaction time, the tube was opened in a N_2-filled glovebox and washed several times with ethyl alcohol to remove any $AgNO_3$ physisorbed on the end basal planes of the sample.

RBS was performed with a collimated beam of $^4He^{2+}$ ions accelerated to an energy of 2.1–2.8 MeV and focused onto a 4-mm^2 spot; 20 μC of charge was collected for each run. A gold–palladium film on Si was used for energy calibration. Data were analyzed with computer software developed at Cornell University.[15] X-ray diffraction patterns were obtained with a Scintag diffractometer (Cu Kα radiation).

Results and Discussion

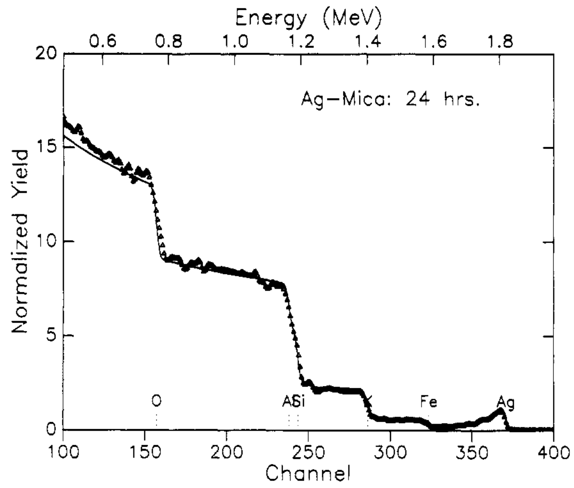

Figure 4. RBS spectrum of mica exposed to $AgNO_3$ at 350 °C for 24 h. The experimental data (triangles) have been simulated (solid line) by using the chemical composition and the diffusion coefficient given in the text.

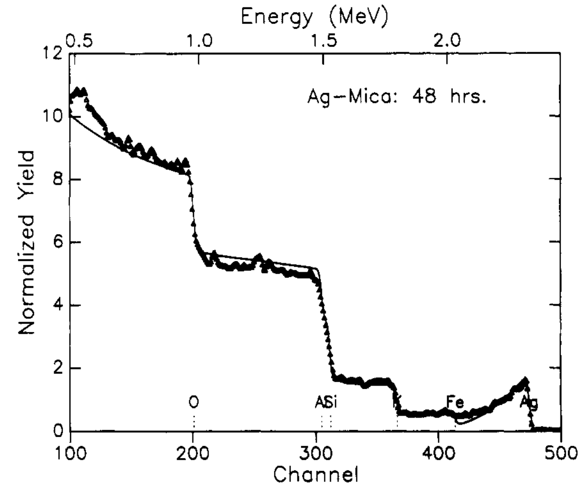

Figure 5. RBS spectrum of mica exposed to $AgNO_3$ at 350 °C for 48 h. Triangles represent experimental data points; the solid line is a computer-simulated spectrum.

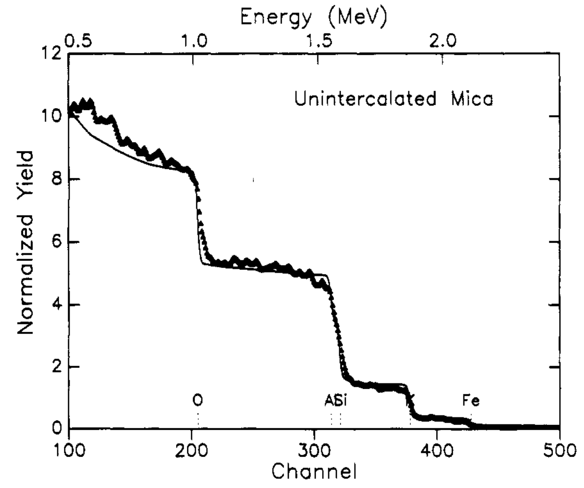

Figure 6. RBS spectrum of pristine mica. Triangles represent experimental data points; the solid line is a computer-simulated spectrum.

The RBS spectra of the muscovite mica sample heated to 350 °C in the presence of $AgNO_3$ for 24 and 48 h are shown in Figures 4 and 5, respectively. For comparison the spectrum of a pristine sample is shown in Figure 6. In the pristine sample, four major steps are observed that correspond to scattering from iron, potassium, silicon/aluminum, and oxygen, respectively. The silicon and aluminum steps are not well resolved in the spectrum because of the closeness of their atomic numbers. The spectra of samples that have been exposed to $AgNO_3$ show, in addition, scattering from Ag. This scattering does not show the same step feature observed for the other elements in the sample, but instead it exhibits a "tail" with the concentration of Ag approaching zero in the interior of the sample. The rapid decrease is characteristic of a concentration gradient wherein the interlayer potassium ions are gradually replaced by silver ions. On the basis of the energy difference between the He^{2+} ions backscattered from Ag^+ at the surface (1.82 MeV, Figure 4) and those beneath the surface where the concentration becomes approximately zero (1.62 MeV, Figure 4), we calculate the

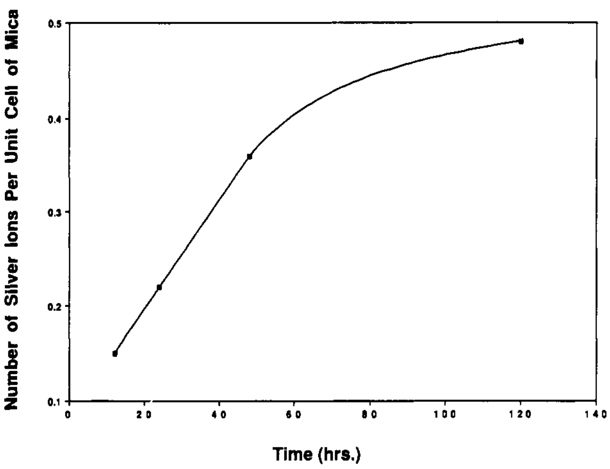

Figure 7. Number of silver ions per unit cell, obtained from RBS simulations, as a function of time.

extent of intercalation to be at least 6500 Å from the end basal plane. Thus, at least, 650 layers have been decorated with silver ions during the first 24 h of exposure. However, the silver concentration, or the extent of ion exchange, decreases from the end basal plane to the interior of the sample.

Using a computer simulation program,[15] we fit the experimental RBS data for pristine mica to $K_2(Al_{3.7}Fe_{0.3})[Si_6Al_2]O_{20}(OH)_4$ (Figure 6). Although we believe that the concentration gradient is not due to transverse diffusion through the end basal planes of the sample, we have, nevertheless, attempted to fit the data using Fick's law. Assuming that C_0 is the concentration of silver at the surface of a semiinfinite solid that is held fixed with time, the diffusion equation has the following form:

$$C(x,t) = C_0 \operatorname{erfc}\,[x/2(Dt)^{1/2}] \tag{6}$$

where x is the depth below the surface, D is the diffusion coefficient, and erfc (x) is the error function complement.[15] From the simulations (Figures 4 and 5) we obtain diffusion coefficients of 5×10^{-15} and 12×10^{-15} cm^2/s for the 24- and 48-h exposed samples, respectively. The corresponding "surface" chemical compositions are $Ag_{0.22}K_{1.8}(Al_{3.7}Fe_{0.3})[Si_6Al_2]O_{20}(OH)_4$ and $Ag_{0.36}K_{1.6}(Al_{3.7}Fe_{0.3})[Si_6Al_2]O_{20}(OH)_4$ for the short and long reaction times, respectively.

Since Fick's law is not obeyed when a local equilibrium is not realized and because of the anisotropic character of the diffusivity, the numbers for the diffusion coefficient represent an estimate and should be used only as such. From the chemical compositions we note that silver is introduced in the sample at the expense of potassium, suggesting an ion-exchange process. The ion-exchange mechanism is further supported by the absence of nitrate ions as evidenced by infrared and nitrogen resonance techniques.[13,17] Since the samples are cut from a single crystal, the external surface area is minimal. Thus, the observed concentration of silver ions is in excess of the amount estimated from the exchange sites on the external surface only.[18] The surface concentration of silver is higher for the longer exposure time, suggesting that a true equilibrium has not been achieved at the surface within the first 24 h of exposure. However, further exposure of the sample only slightly increases the silver "surface" concentration. After 120 h, 0.48 Ag ion/unit cell has been incorporated. This corresponds to about one-quarter of the potential ion-exchange sites. The "surface" concentration of silver, as determined from the RBS spectra, appears to increase linearly with time during the early stages of the reaction, but a plateau is reached at longer reaction times (Figure 7).. This plateau is probably due to the difference in size between the two cations as well as the layer rigidity of the host (vide infra), which impede the process.

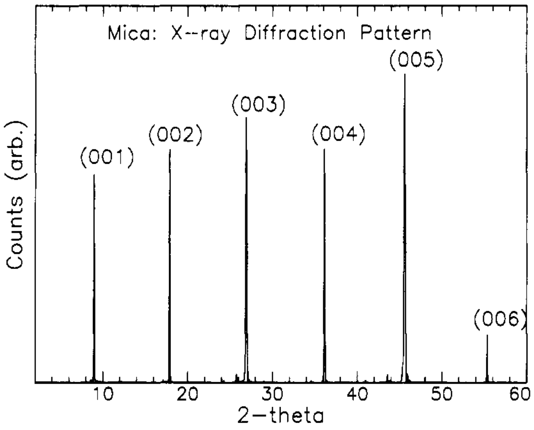

Figure 8. X-ray diffraction pattern of pristine mica.

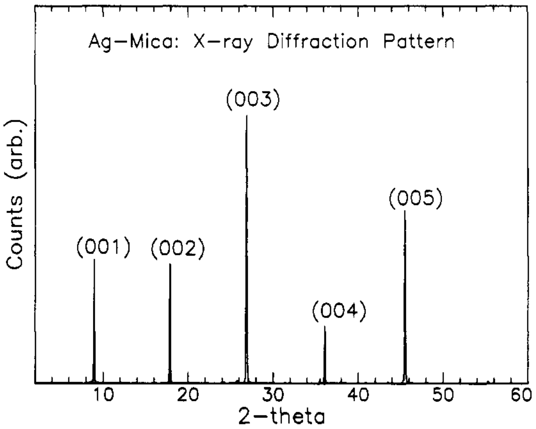

Figure 9. X-ray diffraction pattern of mica after exposure to $AgNO_3$ at 350 °C for 120 h.

X-ray diffraction patterns of the pristine and $AgNO_3$-exposed mica for 120 h are shown in Figures 8 and 9, respectively. Although the basal spacing remains virtually the same, the intensities of the Bragg peaks are dramatically altered upon partial substitution of potassium with silver cations. The out-of-plane correlation length ξ, defined by $\xi = 2/\Delta q$ where Δq is the fwhm of a Bragg peak,[6] is 330 and 285 Å for the pristine and 120-h-exposed samples, respectively. The difference in X-ray diffraction patterns is attributed to the in-plane disorder as a result of the partial replacement of potassium with silver cations in the mica galleries.

On the basis of the above experimental evidence we are proposing the following intercalation mechanism: at first, silver replaces some of the potassium ions on the end basal planes of mica. The decoration of the end basal plane with silver ions "activates" the next layer, initiating the ion-exchange process in that layer (Figure 10). Once a certain concentration of silver is reached, the next layer is activated and the effect is transferred through the successive layers. This mechanism is similar to that observed in intercalation of graphite.[9,10] The ion-exchange process in each layer continues even after the effect is transferred to

---

(17) Resonance techniques exhibit enhanced sensitivity compared to RBS, especially for light elements such as O, N, and C.

(18) Solomon, D. H.; Hawthorne, D. G. *Chemistry of Pigments and Fillers*; Wiley: New York, 1983; p 20.

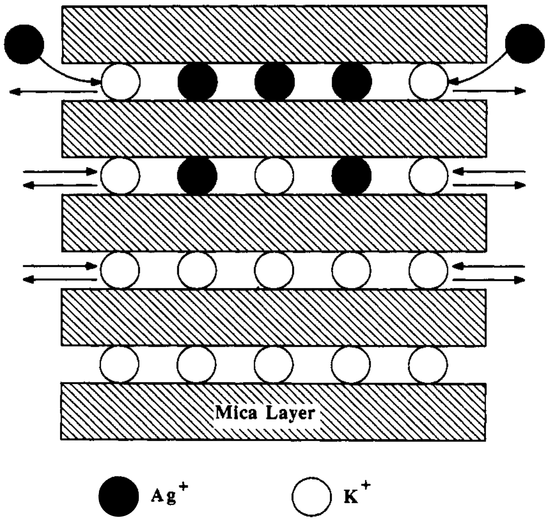

Figure 10. Schematic showing the proposed ion-exchange mechanism. Successive layers are decorated by silver ions that are introduced through the periphery of the sample.

the next layer until an equilibrium concentration is reached. Since activation of successive layers is a critical step in the mechanism, a concentration gradient normal to the layers is observed.

An alternative reaction mechanism in which the observed concentration profile is solely due to diffusion of silver ions from the end basal planes through defects and dislocations in the crystal was ruled out, since we found that the concentration of silver was consistently higher at the edges than at the center of the sample. Thus, it appears that the silver ions are introduced in the galleries through the periphery of the sample as expected for an anisotropic two-dimensional crystal. Therefore, though at room temperature the potassium ions are "locked" into the ditrigonal cavity formed by the oxygen atoms of the tetrahedral layer,[19] at higher temperatures the cations gain some mobility allowing for cation exchange to take place. However, due to the strong bonding between the cations and the surrounding oxygen atoms in mica we expect the in-plane diffusion to be relatively slow compared to the more accessible galleries in MTSs.

The basal spacing in mica is determined by the size of the gallery cations and their relative position with respect to the oxygen atoms in the tetrahedral sheets.[20] Furthermore, the size of the ditrigonal cavity in which the cations rest is controlled by the in-plane rotational distortion of the oxygen atoms in adjacent tetrahedra.[4,21,22] To avoid "sagging" of the layers caused by the partial substitution of potassium with the smaller silver ions (the differential height is 0.4 Å),[23] the tetrahedral rotation angle needs to be increased.[22] The different tetrahedral rotation angles will result in lateral disorder as well as different gallery heights. As a result, the ion-exchange process is countered by the energy required for the in-plane rotational distortion. Due to the small fraction of potassium cations been replaced by silver ions, we observe no measurable change in the basal spacing. However, significant changes in the relative intensities of the diffraction peaks accompanied by a change in the out-of-plane correlation length are observed. Since both the degree of distortion in the tetrahedral layer and the vapor pressure of the intercalant are expected to be affected by temperature, we anticipate the intercalation process to be temperature dependent. Experiments are in progress to investigate the dependence of the extent of intercalation on temperature.

Conclusions

The most striking results from the above experiments are the demonstration of ion exchange in muscovite mica and the concentration gradient observed for the silver ions. Although substitution of the potassium ions is incomplete, at least at the reaction temperature used in this experiment, a whole family of layered structures already considered inert are now available for future experiments. This offers new opportunities given that micas are widely available from natural sources as single crystals.

Acknowledgment. This work was sponsored by the National Science Foundation (DMR-8818558) through the Materials Science Center at Cornell. S. A. Solin and M. S. Whittingham are acknowledged for helpful discussions.

Registry No. $AgNO_3$, 7761-88-8; muscovite, 1318-94-1.

---

[19] Whittingham, M. S. *Solid State Ionics* **1987**, *25*, 295.

[20] Lin, C.; Bailey, S. W. *Am. Mineral.* **1984**, *69*, 122.

[21] York, B. R.; Solin, S. A.; Wada, N.; Raythatha, R.; Johnson, I. D.; Pinnavaia, T. J. *Solid State Commun.* **1985**, *54*, 475.

[22] Radoslovich, E. W.; Norrish, K. *Am. Mineral.* **1962**, *47*, 599.

[23] Cotton, F. A.; Wilkinson, G. *Advanced Inorganic Chemistry*; Interscience: New York, 1972.